JACS
JOURNAL OF THE AMERICAN CHEMICAL SOCIETY

COMMUNICATION

pubs.acs.org/JACS

Direct Conversion of Bio-ethanol to Isobutene on Nanosized $Zn_xZr_yO_z$ Mixed Oxides with Balanced Acid−Base Sites

Junming Sun,[†] Kake Zhu,[†] Feng Gao,[‡] Chongmin Wang,[†] Jun Liu,[†] Charles H. F. Peden,[†] and Yong Wang*[,†,‡]

[†]Institute for Interfacial Catalysis, Pacific Northwest National Laboratory, Richland, Washington 99352, United States

[‡]The Gene & Linda Voiland School of Chemical Engineering and Bioengineering, Washington State University, Pullman Washington 99164, United States

Supporting Information

ABSTRACT: We report the design and synthesis of nanosized $Zn_xZr_yO_z$ mixed oxides for direct and high-yield conversion of bio-ethanol to isobutene (~83%). ZnO is addded to ZrO_2 to selectively passivate zirconia's strong Lewis acidic sites and weaken Brönsted acidic sites, while simultaneously introducing basicity. As a result, the undesired reactions of bio-ethanol dehydration and acetone polymerization/coking are suppressed. Instead, a surface basic site-catalyzed ethanol dehydrogenation to acetaldehyde, acetaldehyde to acetone conversion via a complex pathway including aldol-condensation/dehydrogenation, and a Brönsted acidic site-catalyzed acetone-to-isobutene reaction pathway dominates on the nanosized $Zn_xZr_yO_z$ mixed oxide catalyst, leading to a highly selective process for direct conversion of bio-ethanol to isobutene.

With increasing demands for energy, concerns about anthropogenically caused global climate change, and depletion of fossil feedstocks, more attention has been paid to alternative and renewable sources for fuels and chemicals. Biomass is considered a CO_2 neutral energy carrier and is one of the most abundant and renewable natural resources. For the past decade, biomass conversion has attracted increasing research interest to produce biofuels, with bio-ethanol being a major product.[1−3] With increased availability and reduced cost of bio-ethanol, conversion of this particular bio-based feedstock to highly valuable fuels and chemicals has been an especially important research goal.[4−6] Currently, research on bio-ethanol conversion to value-added chemicals focuses mainly on ethanol dehydration to ethylene, or ethanol dehydrogenation to acetaldehyde and then to acetone via Aldol-condensations pathways ($2CH_3CHO \rightarrow CH_3CHOHCH_2CHO \rightarrow CH_3COCH_2CHO + H_2O \rightarrow CH_3COCH_3 + CO_2 + H_2$).[5] Research on direct bio-ethanol transformations to other types of highly valuable fuels and chemicals has not been carried out. In large part, this is due to the fact that such a process requires catalysts with multiple functions in order to yield more valuable chemicals such as isobutene. Isobutene is of special interest because it is widely used as an intermediate for the production of a variety of industrially important products. For example, the trimerization of isobutene produces tri-isobutenes,[7] which can be used as a premium (odorless, no aromatics) solvent and as an additive for jet fuel. Isobutene dimerization and hydrogenation to produce isooctane is used to increase the octane number of gasoline,[8] and butyl rubber is produced from isobutene polymerization.[9] Isobutene also reacts with alcohols such as ethanol to form ethyl *tert*-butyl ether (ETBE), a gasoline additive.[10] Currently, isobutene is obtained from catalytic or steam cracking of fossil feedstocks.[11] With the depletion of fossil resources and increased demand for the isobutene market, it is desirable to explore alternative routes to synthesize isobutene from renewables.

Basic catalysts, such as ZnO-CaO, ZnO-Fe_2O_3, etc., can be used to convert ethanol to acetone (eqs 1 and 2),[5,12,13] while selective conversion of acetone to isobutene (eq 3) is efficiently accomplished with special structured acidic zeolites.[14−16] It is expected that mixed oxide catalysts with balanced acid−base sites could make a direct conversion of ethanol to isobutene possible. Unfortunately, there have been no reports on the direct conversion of ethanol to isobutene (eq 4).

$$CH_3CH_2OH \rightarrow CH_3CHO + H_2 \quad (1)$$

$$2CH_3CHO + H_2O \rightarrow CH_3COCH_3 + CO_2 + 2H_2 \quad (2)$$

$$3CH_3COCH_3 \rightarrow 2\ i\text{-}C_4H_8 + CO_2 + H_2O + H_2 \quad (3)$$

$$3CH_3CH_2OH + H_2O \rightarrow i\text{-}C_4H_8 + 2CO_2 + 6H_2 \quad (4)$$

Herein, in connection with rapid advancement of processes for biomass conversion to bio-ethanol, we report a new process for direct conversion of bio-ethanol to isobutene (defined here as ETIB) by balancing the strength and distribution of both acidic and basic sites on a nanosized $Zn_xZr_yO_z$ mixed oxide catalyst. In experiments performed to date, isobutene yields as high as 83% have been reached, with acetone and hydrogen, both being still valuable, as byproducts.

To incorporate the multiple functionality needed for a catalytic conversion process that directly converts bio-ethanol to isobutene, a number of zinc/zirconium mixed oxide materials ($Zn_xZr_yO_z$) were prepared. The physical properties of these catalyst materials will be described first.

ZrO_2, ZnO, and $Zn_xZr_yO_z$ mixed oxides with varying Zn/Zr ratios, unless otherwise noted, were prepared by a modified hard-template method[17] and characterized by XRD, TEM, and surface area/pore volume measurements. Broad X-ray diffraction peaks for ZrO_2, characteristic of the tetragonal phase, were observed

Received: May 9, 2011
Published: June 17, 2011

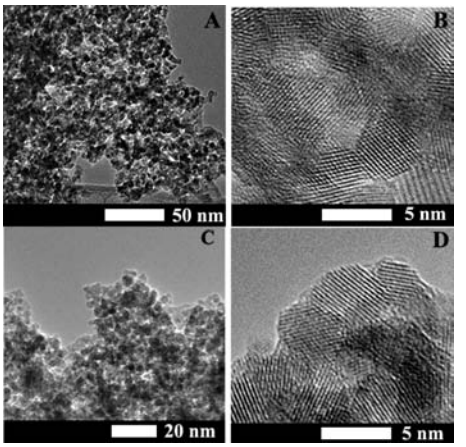

Figure 1. TEM/HRTEM images of (A, B) $Zn_1Zr_{10}O_z$ and (C, D) $Zn_1Zr_{4.6}O_z$.

(Figure S1). For $Zn_1Zr_{10}O_z$ and $Zn_1Zr_{4.6}O_z$, the diffraction peaks of ZrO_2 are further broadened, yet no new diffraction peaks corresponding to ZnO could be detected, suggesting that ZnO and ZrO_2 are well mixed at such low zinc contents. Only at very high zinc contents (e.g., $Zn_1Zr_1O_z$) can broad shoulder peaks from the hexagonal phase of ZnO be resolved. For ZnO, only the hexagonal phase was observed.

TEM/HRTEM results reveal that all $Zn_xZr_yO_z$ catalysts are aggregates of <10 nm-sized particles with a highly crystalline structure (Figure 1). A typical STEM image and the corresponding elemental mapping of $Zn_1Zr_{4.6}O_z$ (Figure S2) further confirmed that ZnO is distributed homogeneously on the ZrO_2 support at lower zinc contents (Zn/Zr ratio less than 1:4), consistent with the XRD observations. However, at Zn/Zr ratios of one or higher, aggregation of a separate ZnO phase could be observed (Figure S3), in agreement with the XRD results.

Nitrogen physisorption results show that all samples except ZnO display large hysteresis loops at relative pressures ranging from 0.9 to 1 (Figure S4), indicating that these mixed oxides have large mesopores which are generated by the voids within and between aggregated nanoparticles.[18] The average pore size for ZrO_2 and $Zn_xZr_yO_z$ mixed oxides calculated from the adsorption branch is between 21 and 25 nm, and their surface area ranges from 138 to 89 m^2/g, depending on the Zn/Zr ratios (Table S1). ZnO has a surface area of 35 m^2/g.

Figure 2A shows the performance of various mixed oxide catalysts for the ETIB reaction. All catalysts showed nearly 100% initial ethanol conversion under the reaction conditions studied. However, the product distributions vary considerably depending on the catalyst composition (Figure 2A). Ethylene is the major product (>95% selectivity) on the pure ZrO_2 support, suggesting that dehydration mainly takes place on the acidic sites of ZrO_2. Conversely, on the basic catalyst, ZnO, acetone is a main product with a selectivity of 66%, along with other minor products, acetaldehyde, CO_2, and ethylene. Most significantly, a substantial amount of isobutene (>40% yield) was observed on the $Zn_1Zr_{10}O_z$ mixed oxide material (Figure 2A), indicating that additional catalytic chemistry is taking place when both acidic and basic sites are present. To the best of our knowledge, direct conversion of bio-ethanol to isobutene with a high selectivity has never been reported. Other catalyst combinations tested here, including basic CeO_2 with acidic ZrO_2 or basic ZnO with acidic ZSM-5, however, do not lead to the formation of a substantial

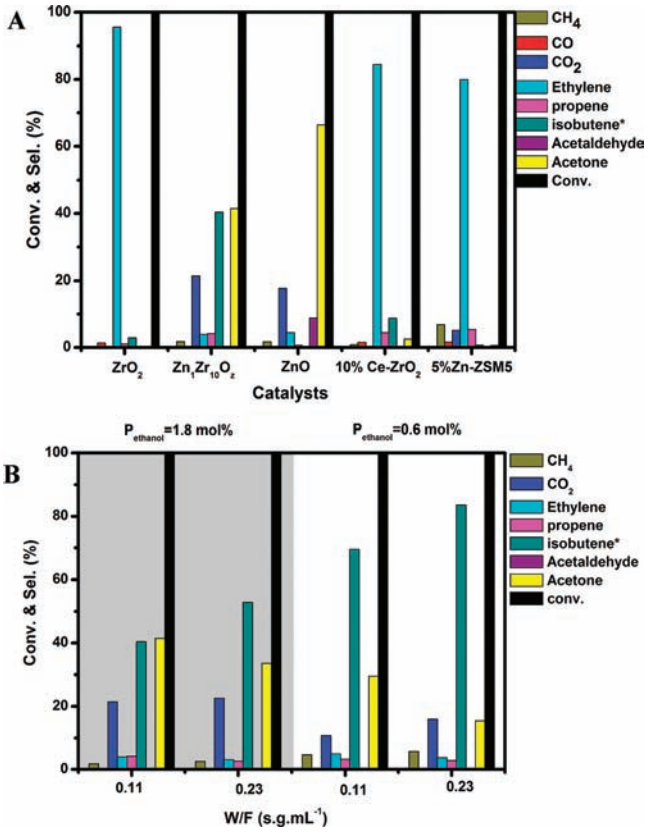

Figure 2. (A) Performance of various acid−base catalyst combinations for the ETIB reaction: 0.1 g of catalyst, 1.8 mol % ethanol, steam to carbon ratio (S/C) = 5, residence time (W/F) = 0.11 $s \cdot g \cdot mL^{-1}$, 450 °C; (B) Performance of the $Zn_1Zr_{10}O_z$ mixed oxide catalyst for the ETIB reaction as a function of gas flow rate and ethanol concentration: 0.1 g of catalyst, S/C = 5, 450 °C. Isobutene* represents isobutene yield.

amount of isobutene, and the product distributions resemble that of ZrO_2 with ethylene being a major product. These observations indicate that unique, multifunctional acid−base properties of the $Zn_xZr_yO_z$ catalyst enable the direct conversion of bio-ethanol to isobutene.

Multiple factors including Zn/Zr ratio, residence time, and reaction temperature were found to affect isobutene selectivity on the $Zn_xZr_yO_z$ mixed oxide catalysts. In particular, selectivity to isobutene increases while acetone selectivity decreases with residence time (Figure 2B), suggesting that acetone is an intermediate in the conversion of ethanol to isobutene. In addition, we found that with an increase in zinc content (i.e., higher Zn/Zr molar ratios), selectivity to acetone increases while selectivity to isobutene decreases (Figure S5). The product distributions were also found to be dependent on reaction temperature. For example, a relatively small decrease of reaction temperature from 450 to 400 °C results in a significant increase in acetone selectivity (from 15% to 58%) at the expense of isobutene selectivity (Figure S6). At a higher reaction temperature (480 °C), acetone selectivity decreased from 15% to 5%, although isobutene selectivity also decreased while H_2 and CO_2 selectivities increased significantly, indicating that ethanol steam reforming dominates at higher temperatures. Importantly, note that isobutene yields as high as 83% were obtained under the most optimum reaction conditions tested in these studies (Figure 2B).

Ethanol conversion to acetone has been widely studied on a variety of basic catalysts.[5,12,13] The reaction mechanism has been proposed to proceed via ethanol dehydrogenation to acetaldehyde (eq 1), followed by a complex aldol-condensation pathway, to form acetone on the basic sites (for overall reaction, see eq 2).[5] The conversion of acetone to isobutene has also been reported on certain structured acidic zeolites. Both surface acidity and microporous structure were found to be critical to suppress polymerization side reactions and thus improve isobutene selectivity.[14−16] The detailed reaction mechanism has been investigated using ^{13}C NMR and was proposed to involve a complex protonization of acetone by a Brönsted acid, followed by condensation and dehydration of protonated acetone to mesityloxide-like species, which then decomposed to form isobutene (for overall reaction, see eq 3).[16] In the new results described here, both ethanol to acetone and acetone to isobutene conversions are shown to occur with high selectivity over nanosized $Zn_xZr_yO_z$ mixed oxide catalysts. We suggest that a delicate balance of acid−base pairs on the $Zn_xZr_yO_z$ mixed oxides provides the acidic sites required to catalyze acetone conversion to form isobutene while still minimizing the undesirable acid-catalyzed ethanol dehydration reaction that forms ethylene. Furthermore, a specific microporous environment, suggested to be important in zeolite catalysts for selectively producing isobutene from acetone, does not appear to be a critical factor in the $Zn_xZr_yO_z$ materials, perhaps due to the moderated Brönsted acidity (to be discussed further below) in these new mixed oxide catalysts.

To unravel the roles of and interplay between ZnO and ZrO_2 during the ETIB reactions, an experiment on physically mixed powders of ZnO and ZrO_2 (10 wt % ZnO + 90 wt % ZrO_2) was performed. This catalyst gave rather complex products including ethylene, propene, acetone, acetic acid, and CO_2, with less than 3% yields of isobutene (Figure S7). The carbon balance, calculated based on the quantification of known products, is less than 70%, indicating that substantial quantities of unknown products are also formed. The low isobutene yield and unknown product formation could be due to acetone polymerization and coking reactions on ZrO_2.[19] Apparently, the close coupling and interplay between zinc and zirconium in the mixed oxide is critical to achieving a high selectivity toward the target product, isobutene.

CO_2 temperature programmed desorption (TPD) and infrared spectroscopic analysis of adsorbed pyridine (IR-pyridine) experiments are widely used to probe the surface acid−base properties of solid catalysts.[20−23] These techniques were used here to better understand the intrinsic acid−base functionalities of the $Zn_xZr_yO_z$ mixed oxides and correlate them with their interesting catalytic behavior. CO_2-TPD experimental results (Figure S8) indicate that the addition of ZnO suppresses both hydroxyls and Lewis acid−base sites on ZrO_2 without generating new acidic−basic sites, consistent with Tanabe's models.[24] Moreover, samples with Zn/Zr ratios of >1/4, i.e. $Zn_1Zr_1O_z$, showed essentially identical CO_2 desorption behavior to that of ZnO (Figure S8), suggesting similar surface properties for both catalysts as confirmed by their similar catalytic performance (Figure S5).

Figure 3 shows the diffuse reflectance infrared Fourier transform spectra (DRIFTS) of adsorbed pyridine on ZrO_2, ZnO, and the $Zn_xZr_yO_z$ mixed oxides. To avoid any influence of physisorbed pyridine, IR spectra of adsorbed pyridine were compared at 350 °C. Both strong Lewis and Brönsted acidic sites (L and B sites) were observed on the nanosized ZrO_2. Based on prior spectral interpretation of adsorbed pyridine on ZrO_2 or

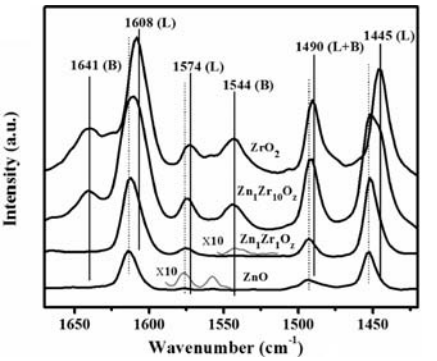

Figure 3. DRIFT spectra of adsorbed pyridine on ZrO_2, ZnO, and the $Zn_xZr_yO_z$ mixed oxides. Physisorbed pyridine was removed by flowing He at 350 °C before IR analysis.

analogues,[22] absorbance bands at 1608, 1574, 1490, and 1445 cm^{-1} can be attributed to pyridine adsorbed on L, L, L+B, and L sites, respectively, while those at 1641 and 1544 cm^{-1} are assigned to protonated pyridine species on B sites. It is worth mentioning that B sites were not detected on ZrO_2 prepared with a traditional precipitation method.[21] The existence of B sites on the nanosized ZrO_2 prepared with the hard template route in this study is likely due to the decreased particle sizes of ZrO_2,[25] as also evidenced in the TEM images (Figure 1). On ZnO, pyridine bands characteristic of adsorption on primarily L sites were observed. However, the intensities of these bands are much lower compared to those on ZrO_2. In addition, all pyridine features on ZnO were found at higher frequencies than their counterparts on ZrO_2, suggesting the much weaker acidity of ZnO relative to ZrO_2. This was further confirmed by the IR analysis of adsorbed pyridine at different temperatures (data not shown). With increasing Zn/Zr molar ratios in the mixed oxides, the intensities of the IR features characteristic of protonated pyridine decrease monotonically. Meanwhile, the intensities of absorbance bands characteristic of pyridine adsorbed on the L sites of ZnO increase at the expense of those on ZrO_2. No additional new bands were observed with the addition of ZnO to ZrO_2. These results suggest that the introduction of ZnO neutralizes both B sites and the stronger L sites on ZrO_2 but does not generate new acidic sites. Thus, the IR-Pyridine results agree well with the CO_2-TPD observations, where decreased CO_2 desorption from both hydroxyl groups (B sites) and strong Lewis acid−base pairs were found with the addition of ZnO in ZrO_2.

Although both acidic and basic sites are present on the ZrO_2,[26] more than 95% of ethanol converts to ethylene (Figure 2A), indicating that strongly acidic sites play a dominating role on this material. Moreover, subsequent formation of isobutene from ethylene was almost unobservable on the pure ZrO_2 support. Therefore, ethylene dimerization/isomerization to form isobutene can likely be excluded as a viable process on these catalysts. On the other hand, on ZnO, acetone is the major product accompanied by a small amount of ethylene (<5% selectivity) (Figure 2A) even though ZnO contains a substantial amount of weaker Lewis acidic sites. This suggests that a basic site-catalyzed dehydrogenation−aldol condensation reaction pathway is predominant on ZnO. It is worth noting that a small amount of isobutene was also formed (yield is less than 0.5% as shown in Figure 2A), likely due to the weak acid sites on ZnO. Clearly, the high isobutene yields on $Zn_xZr_yO_z$ mixed oxides (as high as 83%, Figure 2B) are due to the unique combination and strength of the basic and acidic sites present on the mixed oxides.

To summarize the implications of the CO_2-TPD and IR-pyridine characterization results of the $Zn_xZr_yO_z$ mixed oxides in this study, formation of the mixed oxide modifies the original acid/base properties of the individual oxide. Most importantly, the modification of surface acid/base properties can be well correlated to their catalytic performance in bio-ethanol conversion. The key conclusions about these correlations are captured in Scheme S1. At a high Zn/Zr ratio of 1 (i.e., $Zn_1Zr_1O_z$), most of the stronger L acid sites and B acid sites on ZrO_2 are passivated (Figure 3). Although significant amounts of weak L acid sites are still present, ethanol dehydration reaction rates on these weak L acid sites must be much lower compared with basic site-catalyzed ethanol dehydrogenation and subsequent aldol-condensation pathways to form acetone,[5] as evidenced by the predominant formation of acetone on ZnO and $Zn_1Zr_1O_z$ (Figures 2A and S5). In addition, isobutene selectivity is very low on $Zn_1Zr_1O_z$, suggesting that subsequent conversion of acetone to isobutene requires B acid sites instead of weaker L acid sites. Consistent with this proposal, B acid sites are known to play a key role in the conversion of acetone to isobutene via mesityloxide-like intermediates.[15,16] As the Zn/Zr ratio decreases, the number of B acid sites increases while passivation of the majority of stronger L acidic sites is still achieved (Figure 3) and, in this way, the isobutene selectivity increases. Thus, the B acid sites do play a key role in the conversion of acetone to isobutene on the $Zn_xZr_yO_z$ mixed oxides as would be expected based on prior studies.[15,16] We conclude that only with a properly balanced number of basic and B acid sites, as well as the passivation of the majority of stronger L acidic sites, as we found in the $Zn_1Zr_{10}O_z$ mixed oxide catalysts, can isobutene be produced directly from bio-ethanol at high yields (Figure 2A). Moreover, longer-term durability tests (not shown) suggest that passivation of the stronger Lewis acid−base pairs by ZnO on $Zn_xZr_yO_z$ mixed oxides is also essential for the suppression of polymerization/coking reactions[19] and thus a factor in further optimization of the novel multifunctional nanosized $Zn_xZr_yO_z$ mixed oxide catalysts described here.

In conclusion, we report the first example of the direct and high-yield conversion of bio-ethanol to isobutene, a value-added intermediate useful for the synthesis of fuels and chemicals, using a multifunctional $Zn_xZr_yO_z$ mixed oxide catalyst. The unique combination of Zn- and Zr-oxides provides a balance of the surface acid−base chemistry in the mixed oxides. We find that, with an appropriate Zn/Zr ratio, most of the stronger Lewis acidic sites of ZrO_2 are selectively passivated and Brönsted acidic sites are weakened by the addition of ZnO. Consequently, undesirable bio-ethanol dehydration reactions are largely suppressed, while the surface basic site-catalyzed ethanol dehydrogenation and aldol-condensation reactions followed by Brönsted acid site-catalyzed acetone to isobutene conversion dominate on the $Zn_xZr_yO_z$ mixed oxides. Passivation of the stronger Lewis acidic sites by ZnO on the $Zn_xZr_yO_z$ mixed oxides also mitigates the polymerization/coking of acetone. In this way, a highly selective (as high as 83% yield) process for direct conversion of bio-ethanol to isobutene on the nanosized $Zn_xZr_yO_z$ catalyst has been achieved.

■ ASSOCIATED CONTENT

Supporting Information. Materials, Experimental procedure, Table S1, Figure S1−S9, Scheme S1. This material is available free of charge via the Internet at http://pubs.acs.org.

■ AUTHOR INFORMATION

Corresponding Author
yong.wang@pnl.gov

■ ACKNOWLEDGMENT

We gratefully acknowledge the US Department of Energy (DOE), Basic Energy Sciences, Division of Chemical Sciences, Biosciences and Geosciences for the support of this work. The research described in this paper was performed in the Environmental Molecular Sciences Laboratory (EMSL), a national scientific user facility sponsored by the DOE's Office of Biological and Environmental Research and located at Pacific Northwest National Laboratory (PNNL). We also thank Dr. Liang Zhang (PNNL) for part of the TEM imaging work. PNNL is operated for the DOE by Battelle Memorial Institute under contract number DE-AC05-76RL01830.

■ REFERENCES

(1) Huber, G. W.; Iborra, S.; Corma, A. *Chem. Rev.* **2006**, *106*, 4044–4098.
(2) Chheda, J. N.; Dumesic, J. A. *Catal. Today* **2007**, *123*, 59–70.
(3) Goldemberg, J. *Science* **2007**, *315*, 808–810.
(4) Deluga, G. A.; Salge, J. R.; Schmidt, L. D.; Verykios, X. E. *Science* **2004**, *303*, 993–997.
(5) Murthy, R. S.; Patnaik, P.; Sidheswaran, P.; Jayamani, M. *J. Catal.* **1988**, *109*, 298–302.
(6) Takahara, I.; Saito, M.; Inaba, M.; Murata, K. *Catal. Lett.* **2005**, *105*, 64–74.
(7) Yoon, J. W.; Chang, J.-S.; Lee, H.-D.; Kim, T.-J.; Jhung, S. H. *J. Catal.* **2007**, *245*, 253–256.
(8) Marchionna, M.; Girolamo, M. D.; Patrini, R. *Catal. Today* **2001**, *65*, 397–403.
(9) Carr, A. G.; Dawson, D. M.; Bochmann, M. *Macromolecules* **1998**, *31*, 2035–2040.
(10) Ancillotti, F.; Fattore, V. *Fuel Process. Technol.* **1998**, *57*, 163–194.
(11) Butler, C.; Nicolaides, C. P. *Catal. Today* **1993**, *18*, 443–471.
(12) Nakajima, T.; Yamaguchi, T.; Tanabe, K. *J. Chem. Soc., Chem. Commun.* **1987**, 394–395.
(13) Nakajima, T.; Nameta, H.; Mishima, S.; Matsuzaki, I.; Tanabe, K. *J. Mater. Chem.* **1994**, *4*, 853–858.
(14) Chang, C. D.; Silvestri, A. J. *J. Catal.* **1977**, *47*, 249–259.
(15) Hutchings, G. J.; Johnston, P.; Lee, D. F.; Williams, C. D. *Catal. Lett.* **1993**, *21*, 49–53.
(16) Dolejsek, Z.; Novakova, J.; Bosacek, V.; Kubelkova, L. *Zeolites* **1991**, *11*, 244–247.
(17) Jacobsen, C. J. H.; Madsen, C.; Houzvicka, J.; Schmidt, I.; Carlsson, A. *J. Am. Chem. Soc.* **2000**, *122*, 7116–7117.
(18) Sun, J. M.; Zhang, H.; Tian, R. J.; Ma, D.; Bao, X. H.; Su, D. S.; Zou, H. F. *Chem. Commun.* **2006**, 1322–1324.
(19) Zaki, M. I.; Hasan, M. A.; Pasupulety, L. *Langmuir* **2001**, *17*, 768–774.
(20) Bachiller-Baeza, B.; Rodriguez-Ramos, I.; Guerrero-Ruiz, A. *Langmuir* **1998**, *14*, 3556–3564.
(21) Nakano, Y.; Lizuka, T.; Hattori, H.; Tanabe, K. *J. Catal.* **1979**, *57*, 1–10.
(22) Wan, K. T.; Khouw, C. B.; Davis, M. E. *J. Catal.* **1996**, *158*, 311–326.
(23) Wang, L. Q.; Zhou, X. D.; Exarhos, G. J.; Pederson, L. R.; Wang, C.; Windisch, C. F. *Appl. Phys. Lett.* **2007**, *91*, 173107-1–173107-3.
(24) Shibata, K.; Kiyoura, T.; Kitagawa, J.; Sumiyosh, T.; Tanabe, K. *Bull. Chem. Soc. Jpn.* **1973**, *46*, 2985–2988.
(25) Chuah, G. K.; Jaenicke, S.; Xu, T. H. *Surf. Interface Anal.* **1999**, *28*, 131–134.
(26) Tanabe, K.; Yamaguchi, T. *Catal. Today* **1994**, *20*, 185–197.